Quantitative Analysis of Copper Oxide Nanoparticle Composition and Structure by X-ray Photoelectron Spectroscopy

Chun-Kwei Wu,[†] Ming Yin,[‡] Stephen O'Brien,[‡] and Jeffrey T. Koberstein*[,†]

Department of Chemical Engineering and Department of Applied Physics and Applied Mathematics,
Materials Research Science and Engineering Center, Columbia University, New York, New York 10027

Quantitative determination of oxide nanoparticle composition and structure by X-ray photoelectron spectroscopy (XPS) has proven difficult for metal oxides because of three factors: some oxide nanoparticles are prone to reduction in the XPS instrument under X-ray illumination in the ultrahigh vacuum (UHV) environment; the nanoparticle structure and integral nature of the XPS technique complicate the data analysis; and the composition is not constant during the finite sampling time required for the XPS experiment. In this report, a method for XPS analysis of core−shell nanoparticle composition and structure is developed to account for these factors quantitatively. The method is applied to characterize the copper-(II) oxide (CuO) surface layer on copper(I) oxide (Cu_2O) nanoparticles as well as the reduction kinetics of Cu^{2+} when held under X-ray irradiation in the XPS chamber. The XPS analysis is aided by the availability of copper oxide nanoparticles with a narrow size distribution. When corrected for the finite sampling time, the results show that the reduction reaction follows a second-order rate law, allowing for determination of the true sample composition by extrapolation to zero X-ray exposure time. The initial thicknesses of the CuO surface layer on 6 and 13 nm diameter nanoparticles are estimated to be 0.5 nm by this procedure.

Introduction

Cuprous oxide (i.e., Cu_2O) is a p-type semiconductor with a direct band gap of 2 eV and a high absorption coefficient, properties that make it a promising material for low-cost photovoltaic cells.[1,2] The $Cu/Cu_2O/CuO$ system is also of current interest because of potential applications as an oxidation catalyst.[3−5] Because high surface area is advantageous in these applications, considerable effort has been directed toward the synthesis of Cu_2O nanocrystals.[6−8] Recently, the oxidation/reduction kinetics of copper oxide nanoparticles were proven favorable with respect to the catalytic conversion of carbon monoxide.[9] The Cu_2O nanoparticles that have been prepared, however, normally present a CuO surface layer that can have a profound influence on properties such as catalytic activity, because the catalytic activity is related to oxidation state. It is therefore of general interest to determine the composition and structure of copper oxide as well as other metal oxide nanoparticles. Unfortu-

nately, direct chemical methods for analysis of copper oxide nanoparticle composition are lacking, and other techniques such as X-ray diffraction (XRD) and high-resolution transmission electron microscopy (HRTEM) images have evidenced only the cubic crystalline structure of Cu_2O, suggesting that CuO is present only on the surface of the nanocrystals as a thin amorphous shell.[6,7] Because HRTEM is unable to image the CuO shell, there is a strong current need for a quantitative technique that is capable of specifying both the structure and composition of copper oxide and other metal oxide core−shell nanoparticles.

In a previous study,[7] we demonstrated that XPS can indeed detect the presence of a CuO surface layer (i.e., a Cu^{2+} peak in the spectrum) on Cu_2O nanocrystals, but no attempt was made to develop a quantitative framework for analysis of the XPS data because of a number of experimental issues that complicate the data analysis. It is known, for example, that exposure of various materials to the ultrahigh vacuum XPS environment can cause chemical changes to occur during the analysis. For example, CuO, TiO_2, and CoO, undergo reduction,[10,11] and a number of polymers dehalogenate, i.e., poly(tetrafluoroethylene) (PTFE), poly(vinylidene fluoride) (PVDF), poly(vinylchloride) (PVC), etc.[12−14] The cause of CuO reduction during the XPS acquisition is most likely exposure of the sample surface to electrons or

* Corresponding author. E-mail: jk1191@columbia.edu.
† Department of Chemical Engineering, Columbia University.
‡ Department of Applied Physics and Applied Mathematics, Columbia University.
(1) Briskman, R. N. *Sol. Energy Mater. Sol. Cells* **1992,** *27,* 361.
(2) Musa, A. O.; Akomolafe, T.; Carter, M. J. *Sol. Energy Mater. Sol. Cells* **1998,** *51,* 305.
(3) Jernigan, G. G.; Somorjai, G. A. *J. Catal.* **1994,** *147,* 567.
(4) Huang, T.-J.; Tsai, D.-H. *Catal. Lett.* **2003,** *87,* 173.
(5) Larsson, P.-O.; Andersson, A. *J. Catal.* **1998,** *179,* 72.
(6) Borgohain, K.; Murase, N.; Mahamuni, S. *J. Appl. Phys.* **2002,** *92,* 1292.
(7) Yin, M.; Wu, C.-K.; Lou, Y.; Burda, C.; Koberstein, J. T.; Zhu, Y.; O'Brien, S. *J. Am. Chem. Soc.* **2005,** *127,* 9506.
(8) Ram, S.; Mitra, C. *Mater. Sci. Eng., A* **2001,** *304−306,* 805.
(9) White, B.; Yin, M.; Hall, A.; Le, D.; Stolbov, S.; Rahman, T.; Turro, N. J.; O'Brien, S. *Nano. Lett.* **2006,** *6,* 2095−2098.

(10) Iijima, Y.; Niimura, N.; Hiraoka, K. *Surf. Interface Anal.* **1996,** *24,* 193.
(11) Hirokawa, K.; Honda, F.; Oku, M. *J. Electron Spectrosc. Relat. Phenom.* **1975,** *6,* 333.
(12) Yoshihara, K.; Tanaka, A. *Surf. Interface Anal.* **2002,** *33,* 252.
(13) Duca, M. D.; Plosceanu, C. L.; Pop, T. *J. Appl. Polym. Sci.* **1998,** *67,* 2125.
(14) Wheeler, D. R.; Pepper, S. V. *J. Vac. Sci. Technol.* **1982,** *20,* 226.

photoelectrons from the X-ray window because the reduction is absent when the X-ray source is turned off and because it can be prevented by applying a bias voltage to the sample.[10] However, some studies claimed that the reduction might be ascribed to photoreaction,[15] thermal and electronic reactions,[16] decomposition of hydrocarbon,[17] or the change of the surface composition in the ultrahigh vacuum system.[18] In any case, the in situ reduction of CuO complicates quantification of the composition of copper oxide nanocrystals.

The goal of this study is to provide a quantitative framework for analysis of core−shell nanoparticle composition and structure with the XPS technique. XPS is applied to follow the in situ reduction of the Cu^{2+} in Cu_2O nanocrystals under UHV measurement conditions. The results are analyzed with a core−shell nanoparticle model to characterize the diameter of the Cu_2O core and the thickness of the CuO shell as a function of X-ray exposure time and to use these data to examine the overall kinetics of the reduction reaction. A procedure is then developed to account for the finite sampling time, the integral nature of the XPS technique, and the spherical nature of the nanoparticles that allows for quantification of the initial nanoparticle composition and determination of the rate law for the overall reduction kinetics.

Experimental Section

The synthesis of the Cu_2O nanocrystals was reported previously.[7] Cu nanocrystals are initially decomposed from copper(I) acetate in high-boiling-point solvents at 270 °C and subsequently oxidized to form highly crystalline Cu_2O. This synthesis procedure is important to the success of the XPS method because it provides nanoparticles with a relatively narrow distribution in size. The XPS experiment was performed on a PHI 5500 XPS system equipped with an Al Kα monochromator X-ray source operating at a power of 350 W. The pressure in the test chamber was maintained below 1×10^{-9} Torr during the acquisition process. Survey scans and high-resolution scans were collected with pass energies of 93.9 and 23.45 eV, respectively. Because insulating systems are subject to charging effects that shift the apparent binding energies, the XPS binding energy was internally referenced to the aliphatic C (1s) peak at 284.6 eV that is primarily associated with the oleic acid ligands on the nanoparticles. The takeoff angle, θ, is defined as the angle between a vector normal to the surface and the vector joining the sample and detector. High-resolution spectra were resolved by fitting each peak with a combination Guassian-Lorentzian function after subtracting the background. Atomic concentrations were calculated by normalizing peak areas to the elemental sensitivity factors contained in the PHI software. The spectral acquisition time, Δt, was 35 min for the 13 nm particles and 48 min for the 6 nm particles.

(15) Wallbank, B.; johnson, C. E.; Main, I. G. *J. Electron Spectrosc. Relat. Phenom.* **1974**, *4*, 263.

(16) Klein, J. C.; Li, C. P.; Hercules, D. M.; Black, J. F. *Appl. Spectrosc.* **1984**, *38*, 729.

(17) Losev, A.; Kostov, K.; Tyuliev, G. *Surf. Sci.* **1989**, *213*, 564.

(18) Arko, A. J.; List, R. S.; Bartlett, R. J.; Cheong, S. W.; Fisk, Z.; Thompson, J. D.; Olson, C. G.; Yang, A. B.; Liu, R.; Gu, C.; Veal, B. W.; Liu, J. Z.; Paulikas, A. P.; Vandervoort, K.; H. Claus; Campuzano, J. C.; Schirber, J. E.; Shinn, N. D. *Phys. Rev. B* **1989**, *40*, 2268.
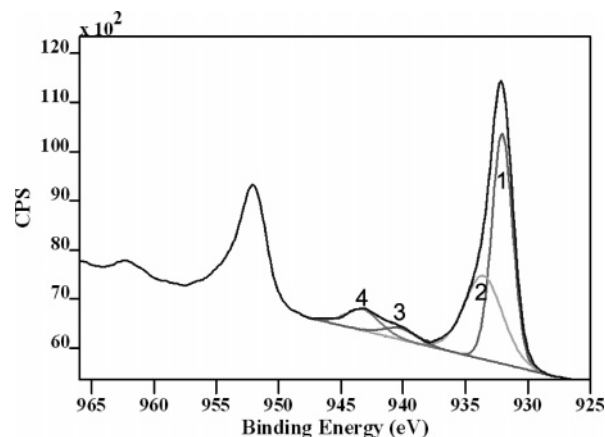
Figure 1. Curve-fitting results for the Cu $2p_{3/2}$ XPS spectrum of 13 nm copper oxide nanoparticles directly after introduction into the XPS chamber.

Results and Discussion

The XPS results reveal the presence of CuO in the Cu_2O nanocrystals, as shown by the Cu $2p_{3/2}$ peaks in Figure 1. Cu^+ has a single peak at 932.2 eV[19,20] (peak 1) with a fwhm of (1.9 ± 0.2 eV[20]), whereas Cu^{2+} has one main peak at 933.5 eV[19,20] (peak 2) with a fwhm of (3.5 ± 0.3 eV[20]) and shakeup satellites (peak 3 and peak 4) at higher binding energies. The shakeup satellites are characteristic of materials having a d^9 configuration in the ground state, i.e., Cu^{2+}.[21] Under X-ray irradiation in UHV, Cu^{2+} is known to undergo reduction. The reduction is usually associated with the formation of Cu^+; however, it is also possible that complete reduction to Cu^0 occurs. Unfortunately, Cu^0 cannot be distinguished from Cu^+ by XPS because of their spectral overlap (i.e., the $Cu2p_{3/2}$ signal for Cu^0 is found at 932.4 eV[19]). The area ratio of peaks 2−4 to that of peak 1 therefore cannot distinguish the exact nature of the reduction reactions, but does serve to characterize the overall in situ reduction of Cu^{2+} in the nanoparticle.[6,10,20]

The reduction of Cu^{2+} induced by the XPS environment is evident in Figure 2. The magnitudes of the main peak and shakeup satellite peaks associated with Cu^{2+} decrease with X-ray exposure time. The combination peak (including contributions from both the Cu^+ peak and main Cu^{2+} peak) also gets narrower with increased reduction. As a control experiment, it was found that little reduction of the Cu^{2+} (Figure 3) occurred for samples placed in the UHV system when the X-ray source was turned off. The reduction is therefore most likely associated with either the action of photoelectrons generated within the sample by X-ray illumination, or electrons emanating from the X-ray window. The carbon:copper ratio remains constant during X-ray exposure, indicating that the oleic acid ligand shell is not degraded as the copper is reduced.

Proper analysis of the XPS time series data can be used to follow the overall reduction kinetics; however, one must

(19) Wagner, C. D.; Riggs, W. M.; Davis, L. E.; Mouler, J. F. *Handbook of X-Ray Photoelectron Spectroscopy*; Muilenberg, G. E., Ed.; Perkin Elmer Corporation, Physical Electronics Division: Eden Prairie, MN, 1979.

(20) Chusuei, C. C.; Brookshier, M. A.; Goodman, D. W. *Langmuir* **1999**, *15*, 2806.

(21) Ghijsen, J.; Tjeng, L. H.; Elp, J. V.; Eskes, H.; Westerink, J.; Sawatzky, G. A.; Czyzyk, M. T. *Phys. Rev. B* **1988**, *38*, 11322.
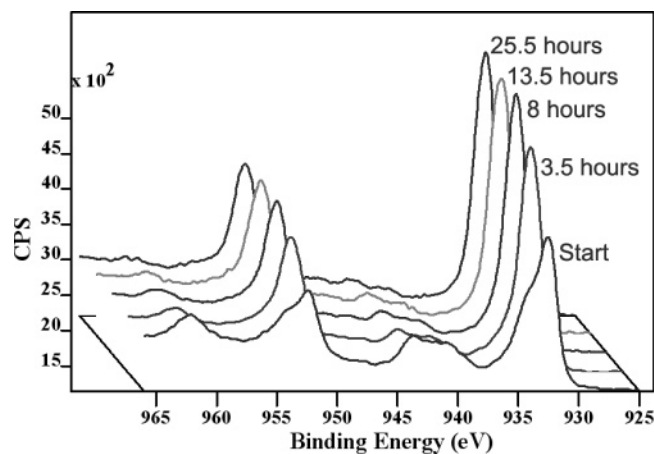
6056   *Chem. Mater., Vol. 18, No. 25, 2006*

Wu et al.

Figure 2. High-resolution XPS spectra showing the effect of X-ray irradiation time on the composition of 6 nm copper oxide nanoparticles.
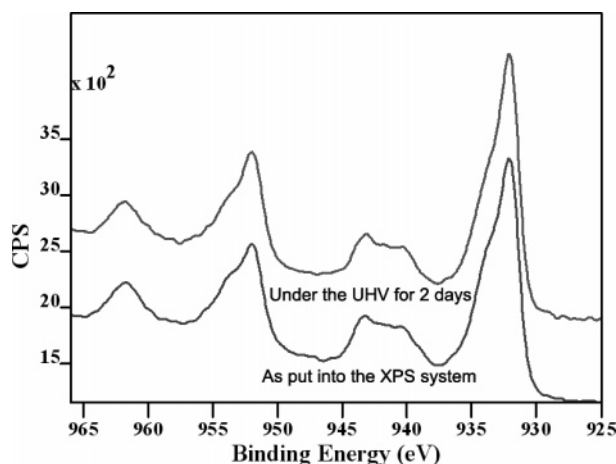

Figure 3. XPS high-resolution spectrum of 6 nm copper oxide nanoparticles after 2 days in the XPS chamber with the X-ray source turned off (upper spectrum); spectrum obtained immediately after insertion into the XPS chamber (lower spectrum).

Figure 4. Second-order rate plot for the reduction of 13 nm copper oxide nanoparticles.

Figure 5. Second-order rate plot for the reduction of 6 nm copper oxide nanoparticles.

correct for both geometric effects associated with the shape of the nanoparticles and the integral nature of the angle-dependent XPS technique. The composition that results from the XPS data does not represent the true composition of the Cu_2O nanocrystals because XPS measures an average composition integrated over the finite sampling depth. The intensity for photoelectrons with a particular binding energy escaping from a flat surface is given by[22]

$$I(\theta) = K \int_0^\infty N(z) \exp\left(\frac{-z}{\lambda \sin \theta}\right) dz \quad (1)$$

where K is the constant related to the elemental sensitivity and instrumental factors, $N(z)$ is the number density of the corresponding atom at depth z, λ is the mean free path of the photoelectrons at that atom's binding energy, and θ is the photoelectron takeoff angle. This relation reflects the fact that the photoelectron yield decreases exponentially with the sampling depth z and that the observed signal for a particular takeoff angle, $I(\theta)$, is a weighted integral of the signals emanating from all sampling depths. A model for the nanoparticle structure, $N(z)$, is therefore required to quanti-
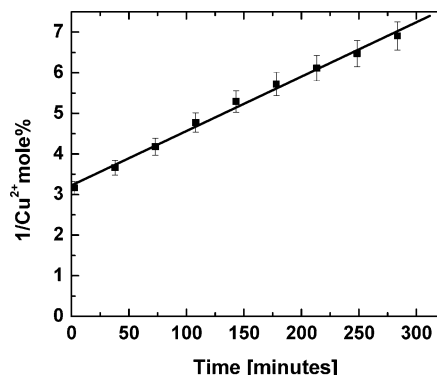
tatively interpret angle-dependent XPS data; otherwise, the contribution from elements nearest to the surface is over-weighted, leading to an erroneous average composition estimate. In the case of the copper oxide nanoparticles, we adopt a core–shell structure with a Cu_2O core and a CuO shell, in fashion similar to that of Sarma et al. for studies on CdS and ZnS nanocrystals.[23,24] For spherical nanoparticles, they showed that a modification of eq 1 for polar coordinates becomes[23,24]

$$I(\theta) = K \int_0^R \int_0^\pi \int_0^{2\pi} N(r) \exp\left(\frac{-f(r)}{\lambda}\right) r^2 dr \sin \theta \, d\phi \quad (2)$$

where R is the nanoparticle radius, and $f(r) = (R^2 - r^2\sin^2\theta)^{1/2} - r\cos\theta$. The integration of ϕ is trivial because of symmetry and leads to a factor of 2π. In the case of a core–shell nanoparticle, a density distribution model is required to represent the atomic radial density function $N(r)$. The model assumes a step density function in the radial direction with two radii: R_1, the radius of the nanoparticle core, and R_2, the nanoparticle radius including the core and shell. In the specific case of spherical Cu_2O nanoparticles with a CuO shell, R_1 is the Cu_2O core radius and $R_2 - R_1$ is the thickness of the CuO shell. The total nanoparticle radius also includes an outer shell of capping ligands (oleic acid) that is assumed to be 1.2 nm thick. The signal originating from the Cu_2O core (i.e., the Cu^+ peak at 932.2 eV; peak 1) is therefore calculated by applying eq 2 with integration limits between 0 and R_1. The signal originating from the CuO shell is

(22) Fadley, C. S.; Baird, R. J.; Siekhaus, W.; Novakov, T.; Bergstrom, S. A. L. *J. Electron Spectrosc. Relat. Phenom.* **1974**, *4*, 93.

(23) Nanda, J.; A.Kuruvilla, B.; Sarma, D. D. *Phys. Rev. B* **1999**, *59*, 7473.
(24) Nanda, J.; Sarma, D. D. *J. Appl. Phys.* **2001**, *90*, 2504.

Table 1. Properties of Cu$_2$O Nanocrystals Determined by Quantitative XPS Analysis[a]

particle diameter[b] (nm)	initial Cu^{2+} concentration (mole %)	core radius (nm)	apparent thickness of CuO layer (nm)	reduction rate constant, k (mole %/min)
6	58.3 ± 1.7	2.49 ± 0.06	0.51 ± 0.06	0.0035 ± 0.0001
13	34.1 ± 0.6	6.00 ± 0.06	0.50 ± 0.06	0.0138 ± 0.0004

[a] Errors are calculated from standard errors in linear regression performed with Origin software, including the effects of error propagation. [b] From TEM analysis.

obtained by applying eq 2 with integration limits between R_1 and R_2. In XPS, it is advantageous to employ intensity ratios rather than individual intensities, as this cancels out certain instrumental factors. In the present case, it allows the effects of the oleic acid ligand shell to be ignored. The intensity ratio of photoelectrons emanating from the Cu$_2$O core to those from the CuO shell can therefore be expressed as

$$\frac{I_{Cu_2O}(\theta)}{I_{CuO}(\theta)} = \frac{K_{Cu_2O}\int_0^{R_1}\int_0^{\pi}\exp\left(\frac{r\cos\theta - \sqrt{R^2 - r^2\sin^2\theta}}{\lambda_1}\right)r^2\sin\theta\, d\theta\, dr}{K_{CuO}\int_{R_1}^{R_2}\int_0^{\pi}\exp\left(\frac{r\cos\theta - \sqrt{R^2 - r^2\sin^2\theta}}{\lambda_2}\right)r^2\sin\theta\, d\theta\, dr} \quad (3)$$

The integrals above cannot be solved analytically and thus were computed numerically with different choices of R_1 and R_2. The average particle size (R_2) was measured by transmission electron microscopy (TEM). The value of R_1 was then varied until the calculated $I_{Cu_2O}(\theta):I_{CuO}(\theta)$ ratio matched that obtained experimentally. Once the two diameters were known, the nanoparticle structure was established and the kinetics of the reduction reaction were quantified. The mean free path of Cu$_2$O (λ_1) and that of CuO (λ_2) are 1.285 and 1.164 nm, respectively, as derived from the NIST Electron Effective-Attenuation-Length Database.[25]

Two different sizes of Cu$_2$O nanocrystals, i.e., 6 and 13 nm in diameter, were used to study the reduction kinetics induced by the X-ray irradiation in the UHV environment. Figures 4 and 5 show that the reduction kinetics correspond well to a second-order rate expression, wherein the Cu^{2+} concentration $C(t)$ is represented as

$$-\frac{dC(t)}{dt} = kC^2(t) \quad (4a)$$

$$\frac{1}{C(t)} = \frac{1}{C_0} + kt \quad (4b)$$

where C_0 is the original concentration of Cu^{2+} and k is the reduction constant with units of mol^{-1} min^{-1}.

The XPS data in Figures 4 and 5 represent time-averaged values over the finite acquisition time and cannot rigorously be compared to eqs 4a and 4b. Instead, the following time-averaged kinetic equations are appropriate

$$\frac{1}{C'(t)}\Delta t = \int_t^{t+\Delta t}\frac{1}{C(t)}dt \quad (5a)$$

$$\frac{1}{C'(t)} = \left(\frac{1}{C_0} + \frac{\Delta t}{2}k\right) + kt \quad (5b)$$

where $C'(t)$ is the time-averaged concentration of Cu^{2+} provided by the XPS data, $C(t)$ is the true concentration of Cu^{2+}, C_0 is the initial concentration at $t = 0$, and Δt is the acquisition time. The kinetics of the overall reduction reactions correspond well to the prediction of eq 5b, as shown in Figures 4 and 5. The initial compositions of the Cu$_2$O nanocrystals before placement into the XPS instrument and the overall reduction rate constants can therefore be estimated from the slope and intercept of linear regressions to the data according to eq 5b. The results of these estimates are given in Table 1. It should be noted that the reduction kinetics monitored in this fashion characterize an overall reduction rate that may include reduction to both Cu$^+$ and Cu^0. Reduction to both species may be expected because the free energies of oxide formation are similar, 35 and 30 kcal/mol for Cu$_2$O and CuO, respectively.[26] The extrapolation to zero time, however, does not contain any contribution from Cu^0, as the initial nanoparticles contain only Cu^{2+} and Cu$^+$.

The initial thicknesses of the CuO layers on 6 and 13 nm diameter Cu$_2$O nanoparticles were both found to be 0.5 nm. The reduction rate constants, however, were found to be dependent on the particle size. Because we are unable to distinguish by XPS whether reduction to Cu^0 occurs, we have no clear mechanistic explanation for this result at the present time. The kinetic fits nonetheless allow for determination of the initial nanoparticle compositions by providing an accurate means to extrapolate the XPS data to zero X-ray exposure time.

Summary

XPS experiments detected the presence of Cu^{2+} in Cu$_2$O nanocrystals; however, the amount observed was found to change during data acquisition because of the in situ reduction of Cu^{2+} under X-ray exposure in the UHV chamber. Quantitative analysis of the composition of the Cu$_2$O nanocrystals as a function of the X-ray exposure time was accomplished by adopting a spherical core–shell model to analyze the XPS data. The overall reduction kinetics of the amorphous CuO layer induced by X-ray irradiation were found to be second order, allowing for determination of the original nanocrystal composition (i.e., after synthesis) by extrapolation to zero time of linear regressions of second-

(25) *NIST Electron Effective-Attenuation-Length Database*, version 1.1; http://www.nist.gov/srd/nist82.htm.

(26) Kim, K. S.; Baitinger, W. E.; Amy, J. W.; Winograd, N. *J. Electron Spectrosc. Relat. Phenom.* **1974**, 5, 351.

order rate plots. The analyses of both 6 and 13 nm particles gave the same thickness for the CuO outer shell (0.5 nm). However, the reduction rate constants differed for reasons that are not clear. The method proposed herein provides an important procedure for determining the composition and structure of Cu_2O nanocrystals and other core−shell nano-particles, especially those prone to in situ reduction in UHV environments.

CM061596D